International Journal of Biological Macromolecules 169 (2021) 428–435

Contents lists available at ScienceDirect

International Journal of Biological Macromolecules

journal homepage: http://www.elsevier.com/locate/ijbiomac

A new biological prospective for the 2-phenylbenzofurans as inhibitors of α-glucosidase and of the islet amyloid polypeptide formation

Giovanna Lucia Delogu [a,1], Benedetta Era [a,1], Sonia Floris [a], Rosaria Medda [a], Valeria Sogos [b], Francesca Pintus [a], Gianluca Gatto [c], Amit Kumar [c], Gunilla Torstensdotter Westermark [d], Antonella Fais [a,*]

[a] Department of Life and Environmental Sciences, University of Cagliari, Monserrato, Cagliari 09042, Italy
[b] Department of Biomedical Sciences, University of Cagliari, Monserrato, Cagliari 09042, Italy
[c] Department of Electrical and Electronic Engineering, University of Cagliari, via Marengo 2, Cagliari 09123, Italy
[d] Disciplinary Domain of Medicine and Pharmacy, Faculty of Medicine, Department of Medical Cell Biology, Uppsala University, Sweden

ARTICLE INFO

Article history:
Received 28 July 2020
Received in revised form 1 December 2020
Accepted 15 December 2020
Available online 19 December 2020

Keywords:
α-Glucosidase
Islet amyloid polypeptide
2-phenylbenzofuran, molecular docking

ABSTRACT

In this study, we have investigated a series of hydroxylated 2-phenylbenzofurans compounds for their inhibitory activity against α-amylase and α-glucosidase activity.
Inhibitors of carbohydrate degrading enzymes seem to have an important role as antidiabetic drugs.
Diabetes mellitus is a wide-spread metabolic disease characterized by elevated levels of blood glucose. The most common is type 2 diabetes, which can lead to severe complications. Since the aggregates of islet amyloid polypeptide (IAPP) are common in diabetic patients, the effect of compounds to inhibit amyloid fibril formation was also determined.
All the compounds assayed showed to be more active against α-glucosidase. Compound **16** showed the lowest IC_{50} value of the series, and it is found to be 167 times more active than acarbose, the reference compound. The enzymatic activity assays showed that compound **16** acts as a mixed-type inhibitor of α-glucosidase. Furthermore, compound **16** displayed effective inhibition of IAPP aggregation and it manifested no significant cytotoxicity.
To predict the binding of compound **16** to IAPP and α-glucosidase protein complexes, molecular docking studies were performed.
Altogether, our results support that the 2-phenylbenzofuran derivatives could represent a promising candidate for developing molecules able to modulate multiple targets involved in diabetes mellitus disorder.

1. Introduction

In diabetic disease, controlling postprandial hyperglycaemia is one of the main therapeutic targets. Inhibition of α-glucosidase (EC 3.2.1.3) and α-amylase (EC 3.2.1.1), which are carbohydrate-hydrolyzing enzymes, is enabled to reduce the rate of glucose absorption and control plasma glucose levels [1,2]. Therefore, in drug discovery α-amylase and α-glucosidase is recognized as an important target [3–5].

The aetiology could be different in diabetes mellitus as well as the treatment, but the hyperglycaemia is the common feature. Chronic hyperglycaemia causes high levels of oxygen free radicals in different tissues of diabetic patients, and plays a significant part in the advancements of various associated complications [6].

Type 1 (T1D) and Type 2 (T2D) diabetes are the two main types of diabetes, and the latter type makes up about 90% of diabetes cases. In over 90% of patients afflicted with T2D, amyloid deposits are observed in the extracellular space of pancreatic islets of Langerhans [7] and intracellular in islet β-cells [8]. The islet amyloid polypeptide (IAPP) is a 37-residue peptide hormone that aggregates to form amyloid fibrils [9], which are seen mainly in association with T2D, but recently also identified in the pancreas of individuals with T1D [10]. Aggregated IAPP has cytotoxic properties and is believed to be of critical importance for the loss of β-cells in T2D [11]. Therefore, the inhibition of its formation has therapeutic potential. Indeed, inhibition approaches of polypeptide-based and of small molecules have provided promising results [12,13].

Benzofuran ring is a basic structure of various natural medicines and synthetic chemicals. Numerous studies have shown that 2-arylbenzofurans have biological activities such as anti-cancer, anti-bacterial, anti-viral, anti-oxidative, anti-fungal, and anti-microbial

* Corresponding author.
E-mail address: fais@unica.it (A. Fais).
[1] These authors contributed equally to this work.

https://doi.org/10.1016/j.ijbiomac.2020.12.117
0141-8130/

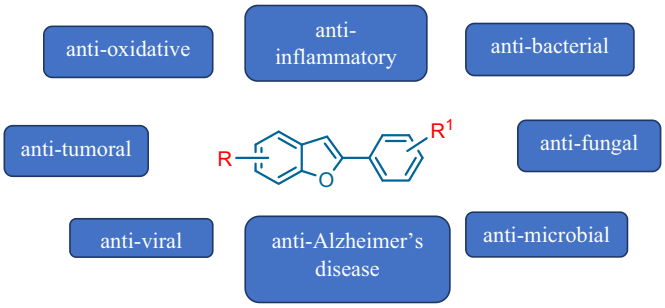

Fig. 1. Biological activities of 2-arylbenzofuran derivatives.

activities (Fig. 1). Thus, there is a great interest in using benzofuran as a building block of pharmacological agents.

Many benzofuran derivatives, of natural or synthetic origin, have been approved clinically, and some of which are fused with other heterocyclic moieties [14].

Keeping in mind that molecules that hit more than one target may possess in principle a safer profile compared to single-targeted ones [15,16], a series of hydroxylated 2-phenylbenzofurans compounds, with promising therapeutic targets [17–19] have been studied. Considering that previous studies [20,21] indicated 2-arylbenzofuran derivatives as antidiabetic agents, we have analysed a series of 2-phenylbenzofuran derivatives, for which the anti-cholinesterase action is already known [16], to improve the potential of this scaffold for their inhibitory activities also towards α-glucosidase and α-amylase enzymes.

Recently, the concept of metabolism-dependent neurodegeneration mechanisms is gaining importance, as T2D patients have a higher risk of developing Alzheimer's disease (AD) symptoms. The overlapping mechanisms of AD and T2D offer a new perspective taking us towards an entirely different approach, which involves targeting insulin signalling, and glucose metabolism as a novel therapeutic strategy for AD [22].

To promote the usage of these inhibitors in drug discovery and development process, their potential effect on the kinetic and structural properties of IAPP have been analysed.

Finally, molecular docking study was performed to spot pivotal structural aspects that influence the activity of compounds against α-glucosidase protein and IAPP.

2. Materials and methods

2.1. Chemistry

All commercial reagents and materials were purchased from commercial sources and used without further purification. Melting points were measured on a Büchi 510 apparatus and were uncorrected. ^{1}H NMR and ^{13}C NMR spectra were recorded with a Varian INOVA 500 spectrometer using deuterated chloroform ($CDCl_3$) and dimethyl sulfoxide (DMSO) as solvents. Chemical shifts (δ) are given in parts per million (ppm) using TMS as an internal standard. Coupling constants *J* are expressed in hertz (Hz). Spin multiplicities were given as s (singlet), d (doublet), dd (doublet of doublets), m (multiplet), and apparent triplet (app t). Using a Perkin Elmer 240B microanalyser, elemental analyses were performed and were found to be 0.4% of calculated values, in all the cases. Column chromatography purifications were performed using Aldrich silica gel (60–120) mesh size. For all compounds, the analytical results revealed 98% purity. We performed flash chromatography (FC) on silica gel (Merck 60, 230–400 mesh); analytical thin-layer chromatography (TLC) was performed on pre-coated silica gel plates (Merck 60 F254), visualized by exposure to UV light.

2.2. Biological assays

2.2.1. Assay for α-amylase inhibitory activity

The inhibition of α-amylase activity by compounds **9–16** was determined by using 2-chloro-4-nitrophenyl-α-D-maltotrioside (CNPG3) as an artificial substrate. The solution containing 60 μL of 50 mM sodium phosphate buffer at pH 7.0, 20 μL of NaCl (1 M) and 40 μL of α-amylase from porcine pancreas (1 mg/mL), was mixed in microplate multi-wells and incubated in the absence or presence of the sample at 37 °C for 10 min. Similarly, acarbose as a standard inhibitor was used as a positive control. Following incubation, we added 80 μL of a 2.5 mM CNPG3 solution and the amount of 2-chloro-nitrophenol released by the enzymatic hydrolysis was monitored at 405 nm.

2.2.2. Assay for α-glucosidase inhibitory activity

Inhibitory activity of α-glucosidase was performed as described by Fais et al. [23]. The solution was prepared in 0.1 M phosphate buffer pH 6.8 and was mixed with 40 μL of enzyme from *Saccharomyces cerevisiae* solution containing 0.125 U/mL.

Twenty microliters of test samples were mixed at various concentrations with the enzyme solution and then incubated for 15 min at 37 °C. After incubation, 20 μL of the substrate, *p*-nitrophenyl α-D-glucopyranoside (pNPG), 5 mM solution in 0.1 M phosphate buffer was added to the above-prepared mixture and incubated again under the same experimental conditions. The subsequent addition of 50 μL of 0.2 M sodium carbonate solution stops the reaction. The amount of released *p*-nitrophenol was measured using a 96-well microplate reader at 405 nm. DMSO control was used whenever required, and the final concentration of DMSO was maintained below 8% v/v, concentration that does not affect the enzyme activity. Acarbose was used as a positive control. The concentration of compound needed to inhibit 50% of α-glucosidase activity under assay conditions was defined as IC_{50} value.

The Lineweaver-Burk double reciprocal plot was performed to determine the mode of inhibition of compound **16** on α-glucosidase. The assay was performed by varying the concentration of inhibitor and pNPG.

2.2.3. Inhibition of IAPP aggregate formation

The formation of amyloid fibril was monitored by characteristic changes in Thioflavin T (ThT) fluorescence intensity. IAPP stock solution was obtained dissolving 2 mg of synthetic IAPP (Cambridge) in 250 μL (2 mM) of hexafluoroisopropanol (HFIP). This stock solution was stored at −20 °C. All solutions for these studies were prepared by adding a PBS buffer thioflavin-T solution (1 mM) to IAPP peptide (in lyophilized dry form) immediately before the measurement. The final concentration of IAPP was 10 μM with 0.5% of DMSO. When compounds were present at different concentration (100 μM, 50 μM, 10 μM, 1 μM, and 0.1 μM), the IAPP to compound ratio was respectively 1:10, 1:5, 1:1, 1:0.1 and 1:0.01 by weight. ThT fluorescence was monitored at 480 nm with 440 nm excitation at 37 °C on a FLUOstar Omega microplate reader. The experiments performed in sextuplicates were repeated three times.

2.2.4. Cell viability assay

HeLa cells viability was detected by the colorimetric 3-(4,5-dimethylthiazol-2-yl)-2,5-diphenyltetrazolium bromide (MTT) assay. These cells were grown in Dulbecco's Modified Eagle Medium supplemented with 10% fetal bovine serum, 2 mM L-Glutamine, penicillin (100 U/mL) and streptomycin (100 μg/mL) at 37 °C in 5% CO_2.

The colorimetric MTT assay was utilized for measuring the activity of mitochondrial enzymes in living cells that converted MTT into purple formazan crystals. Briefly, 3×10^4/mL cells were seeded in a 96-well plate and incubated with samples at concentrations ranging from 1 to 100 μM for 48 h. Since DMSO was used as a solvent for compounds, cell viability was also performed in the presence of DMSO alone, as solvent control. After incubation time, MTT solution (final concentration of 0.5 mg/mL) was added to each well and incubated for 3 h at 37 °C.

The cells were lysed with 100 μL of DMSO (≥99,7%), and the optical density was measured at 560 nm with an auto microplate reader (Multiskan FC - Thermo Scientific). The mean values and standard deviations (SD) were calculated from triplicates.

2.3. Molecular docking

The three-dimensional (3D) structure of IAPP [24] was obtained from the protein data bank (PDB id: 2L86). However, due to the unavailability of the experimental 3D structure of an α-glucosidase protein from *Saccharomyces cerevisiae*, a template-based homology modelling approach was followed using Swiss-model web server [25] with 3D reference structure of isomaltase from *Saccharomyces cerevisiae* (3AJ7) [26] having 72% sequence identity [27] with the target protein structure. The predicted protein tertiary structure model was evaluated by local quality estimates [28] and Ramachandran plot of the dihedrals (see ESI† Fig. S1). The 3D structure of compound **16** was obtained using open-babel software [29]. Further details of ligand preparation have been described in our previous studies [30,31]. The docking experiment to generate a protein-ligand complex was performed using a COACH-D web-server [32].

2.4. Statistical analyses

Statistical differences were evaluated using Graph Pad Version 8 software (San Diego, CA, USA). Comparison between groups was estimated by one-way analysis of variance (one-way ANOVA) followed by Tukey's multiple comparison test. The values with $p < 0.001$ were considered significant. Data displayed are as mean ± SD of three independent experiments.

3. Results and discussion

3.1. Chemistry

Synthesis of 2-phenylbenzofurans was performed using an intramolecular Wittig procedure, primarily due to its simplicity and accessibility [33–35].

The synthesis of 2-substituted benzofurans **1–8** was carried out by Wittig reaction, following the procedure shown in Fig. 2.

Starting with the conveniently substituted 2-hydroxybenzyl alcohols **a-b** and $PPh_3 \cdot HBr$ in acetonitrile, at 82 °C, for 2 h

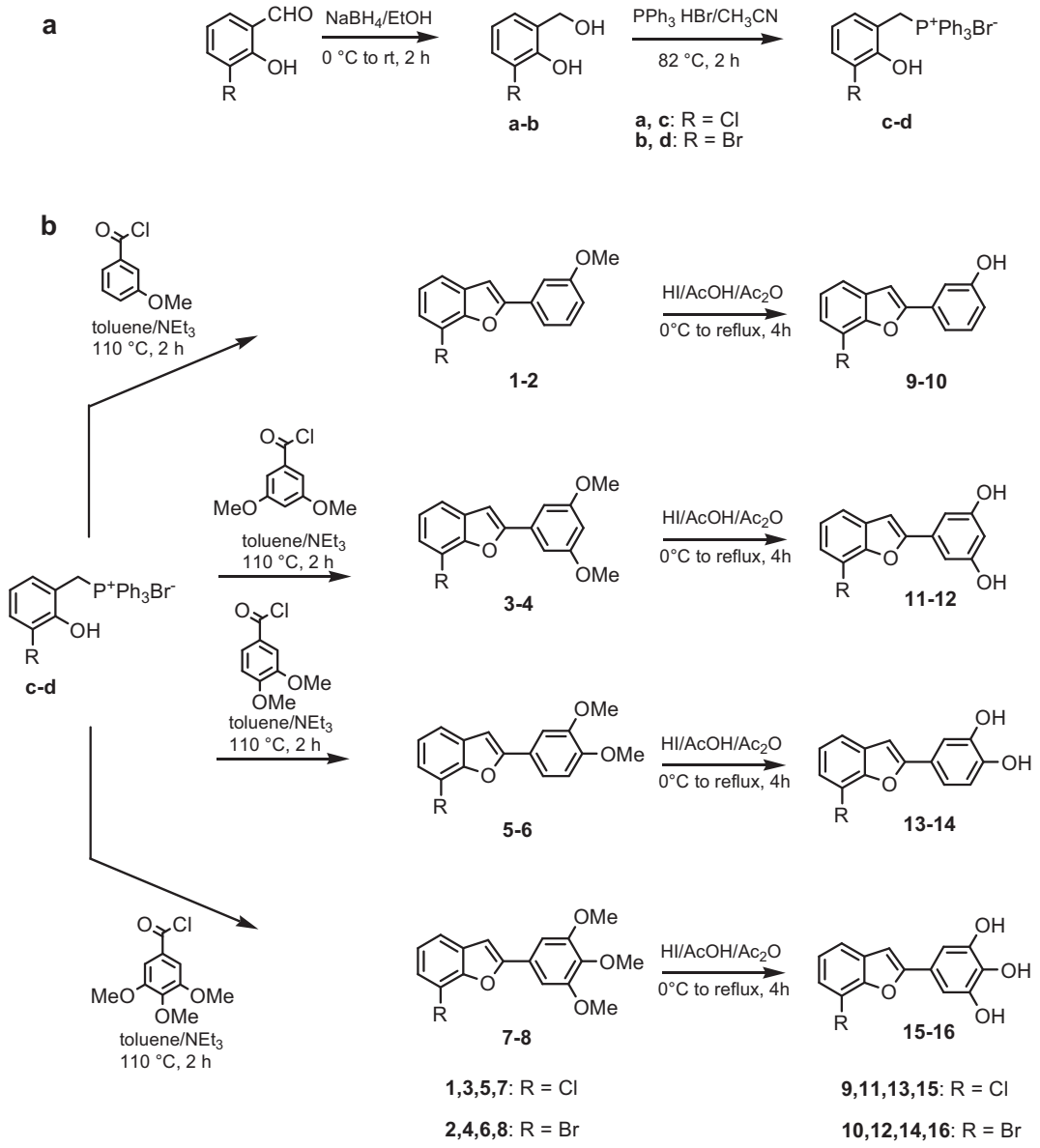

Fig. 2. The synthetic route towards methoxylated 2-phenylbenzofurans **1–8** and hydroxylated 2-phenylbenzofurans **9–16**.

(Fig. 2a), the desired Wittig reagents were readily prepared. The means for the development of the benzofuran moieties **1–8** were accomplished through an intramolecular reaction between the appropriate 2-hydroxybenzyltriphosphonium salt **c-d** and the commercially obtainable benzoyl chlorides, in toluene, at 110 °C, for 2 h. To obtain the corresponding hydroxy derivatives compounds **9–16** (Fig. 2b), hydrolysis of methoxy groups of compounds **1–8** was carried out through the treatment with hydrogen iodide in acetic acid/acetic anhydride at 0 °C and then at reflux for 3 h [18,19] (see ESI† Spectrum S1 and S2).

3.2. Enzyme inhibitory studies

The compounds **9–16** were evaluated for their inhibitory activity against α-amylase and α-glucosidase activity. All the compounds, at a concentration of 25 μM, were weak inhibitors of α-amylase giving 33% of inhibition at most (data not shown). While, at the same concentration, compounds efficiently inhibited α-glucosidase activity, and the results are summarized in Table 1.

Table 1
Inhibition of α-glucosidase enzyme by compounds **9–16**.

Compounds	α-Glucosidase IC_{50} (μM) ± SD
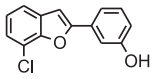 **9**	61.03 ± 0.64[a]
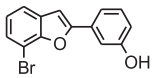 **10**	57.16 ± 3.56[a]
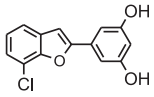 **11**	53.25 ± 1.30[a]
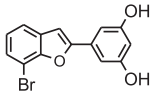 **12**	32.37 ± 2.21[b]
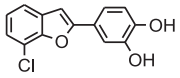 **13**	9.57 ± 3.04[c]
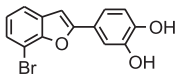 **14**	1.45 ± 0.16[c]
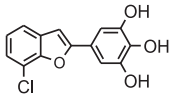 **15**	5.19 ± 0.36[c]
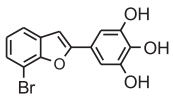 **16**	0.83 ± 0.16[c]
Acarbose[$]	139 ± 11.3[d]

IC_{50} values are expressed as the mean ± SD of three experiments. Different letters indicate statistically significant differences between compounds ($p < 0.001$).
[$] Positive control.

We noted that the compounds with one hydroxyl substituent in meta position of the phenyl ring, and chlorine or bromine atom in position 7 of benzofuran scaffold (compounds **9** and **10**) exerted a weak α-glucosidase inhibitory activity when compared to other compounds. Nevertheless, their IC_{50} values are better than the value determined for acarbose (139 μM), the reference compound. Interestingly, introduction of another hydroxyl group into the other meta-position (compounds **11** and **12**) of the phenyl ring increases the inhibitory activity, which is higher for the compound **12** with an IC_{50} value 4.3-fold better than the reference. It is worth highlighting that the presence of two hydroxyl groups in the meta and para-positions, compounds **13** and **14**, significantly increased the inhibitory activity of the 2-phenylbenzofuran scaffold with an IC_{50} value of 9.57 ± 3.04 and 1.45 ± 0.16 respectively. Compounds **15** (IC_{50} = 5.19 ± 0.36) and **16** (IC_{50} = 0.83 ± 0.16), with three hydroxyl substituents in phenyl ring (3,4,5-positions), inhibited the enzyme with efficiency similar to compounds **13** and **14**. Interestingly, α-glucosidase inhibitory activity displayed by compound **16** was about 167 times higher than the reference compound.

Thus, it establishes that number of hydroxyl groups and their position in the 2-phenyl ring of the synthesized compounds could decrease or increase the inhibitory activity of compounds against α-glucosidase. Our results are in good agreement with other previous studies [19,36], which have shown that the position and number of the hydroxyl groups in the ligand can influence the magnitude of hydrogen bond interactions with the protein, and consequently, their activity.

The mode of inhibition of compound **16** was determined by the Lineweaver-Burk plot, as shown in Fig. 3. Increasing the concentration of compound **16** resulted in a family of lines with different slope and intercept, intersecting in the second quadrant. Thus, implying that compound **16** was a mixed-type inhibitor, which can bind the free enzyme and the enzyme-substrate (ES) with different equilibrium constants, KI and KIS (0.83 and 3.55 μM, respectively). The equilibrium constants values were obtained from the slope or the vertical intercept versus inhibitor concentration, (see ESI† Fig. S2).

3.3. Inhibition of IAPP fibril formation

To monitor the in vitro fibril formation, Thioflavin T (ThT) binding assay has been used. When ThT binds to amyloid fibrils, it exhibits an

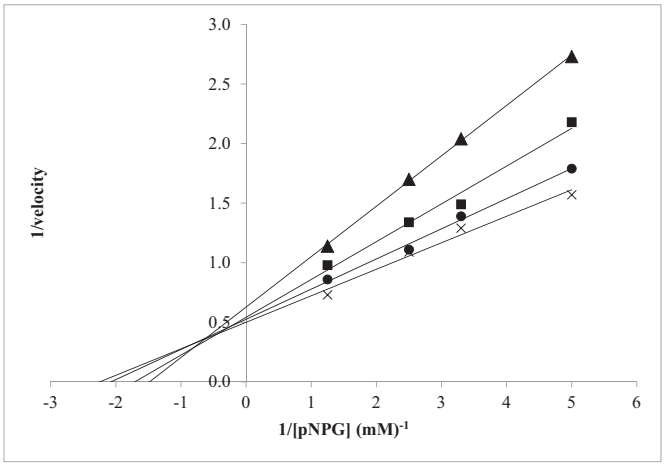

Fig. 3. Lineweaver–Burk plots analysis of compound **16**. Inhibitor concentrations were 0 (X), 0.4 μM (•), 0.6 μM (■), 0.8 μM (▲).

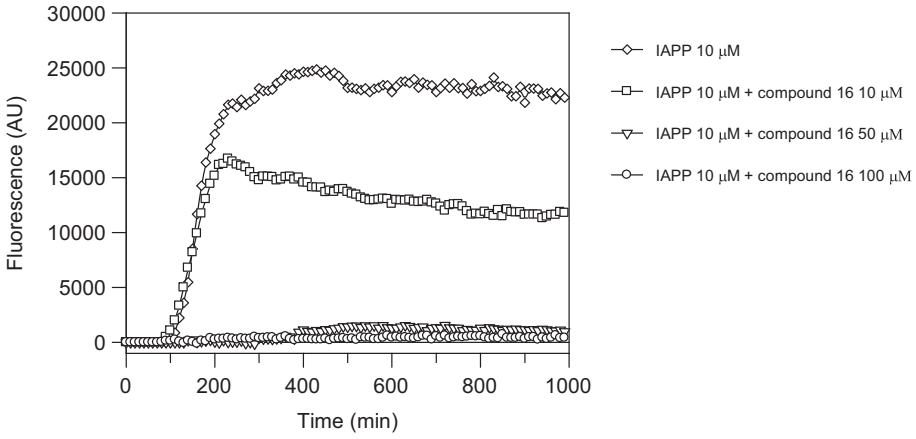

Fig. 4. Thioflavin T fluorescence emission plot corresponding to the β-sheet formation of IAPP samples upon incubation with compound **16**.

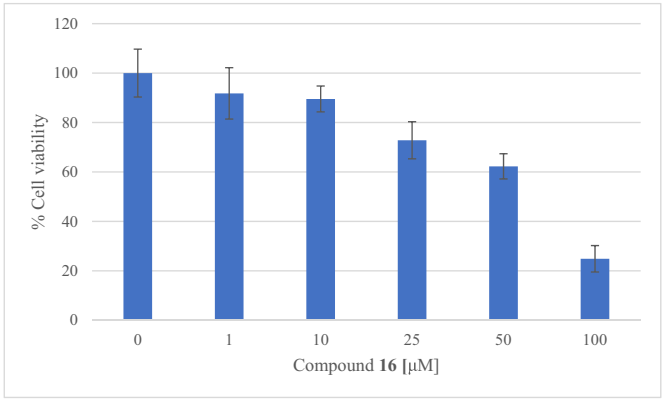

Fig. 5. The effect of compound **16** on HeLa cell viability. Cells were treated with different concentrations of compound (1–100 μM), and their viability was evaluated by MTT assay. Data depict the mean (±standard deviation) of three independent experiments.

enhanced fluorescence and a characteristic blue shift in the emission spectrum.

The fluorescence intensities of the dye were measured as a function of time, and the corresponding spectrum was recorded. Any deviation from the positive control sample along the time scale indicates inhibition or activation of the aggregation processes.

Compounds **9–16** were tested for their ability to inhibit amyloid fibril formation. We added the compounds at the different ratios to IAPP solutions and monitored the kinetics of IAPP amyloid formation by ThT fluorescence emission.

Co-incubation of IAPP at different concentrations with each compound **9–12** did not show any deviation from IAPP alone in ThT fluorescence intensity, and results are comparable (data not shown). The rate of fibril growth does not appear to be significantly affected by these compounds.

Interestingly, the influence of compounds **13–16** on IAPP aggregation is almost opposite to that shown by compounds **9–12**. Indeed, the compounds prevented any increase in ThT signal, reflecting complete prevention of aggregation, and the inhibiting effect lasted for a prolonged time (>150 h). Compound **16**, which displayed the best inhibitory activity against the α-glucosidase enzyme, also resulted as an

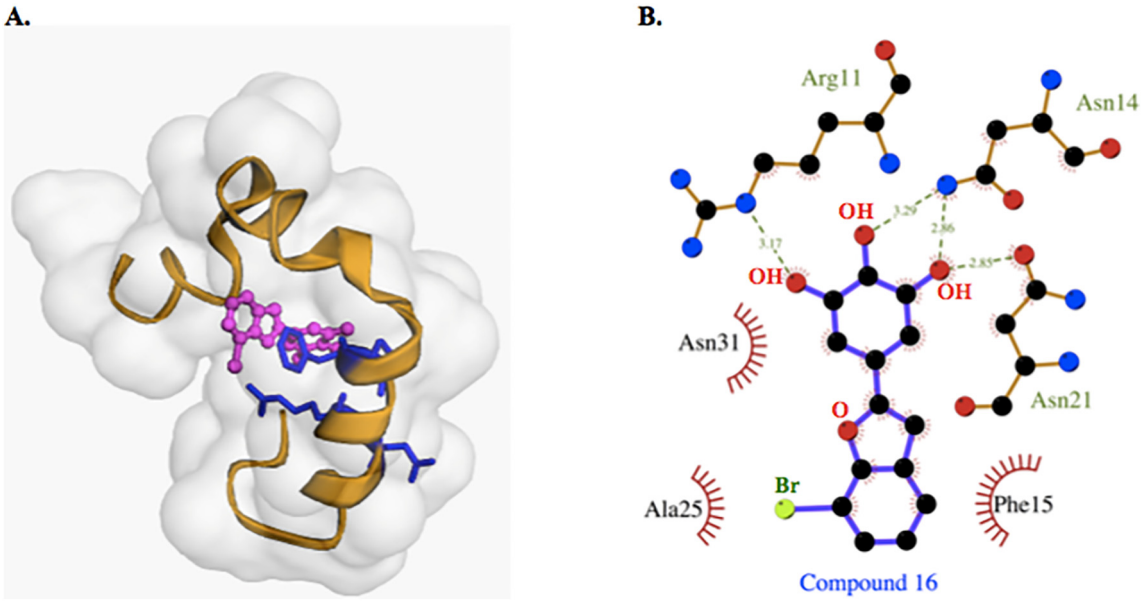

Fig. 6. IAPP-Compound **16** complex. A. The top docked conformation of compound **16** to IAPP. The IAPP is shown as molecular surface and cartoon representation, ligand (magenta) in ball-stick representation and the participating residues (blue) in licorice. B. Compound **16** interactions with the residues of IAPP mediated by hydrogen bonds (H-bonds), and by hydrophobic (H-phobic) contacts. H-bonds are indicated by dashed lines between the atoms involved, while H-phobic contacts by an arc with spokes radiating towards the participating ligand atoms, obtained using Ligplot [37].

effective inhibitor of IAPP aggregation at a concentration of 50 μM (Fig. 4).

3.4. Cell viability

After obtaining encouraging results from the assay experiments, the potential cytotoxicity effect of the promising compound **16** was further evaluated using the MTT test. Hela cells were treated with compound **16** at concentrations ranging from 1 to 100 μM for 48 h, and the potential cytotoxic effect was determined.

Results indicate that compound **16** exhibited no significant cytotoxicity at the concentration in which α-glucosidase activity is inhibited (Fig. 5).

3.5. Molecular and physicochemical properties of compound *16*

The tertiary structure of human IAPP was obtained from protein data bank (PDB id: 2L86), while for the α-glucosidase protein from *Saccharomyces cerevisiae* was generated using homology modelling approach, using the tertiary template structure (PDB id: 3AJ7) of isomaltase. Compound **16** was docked alternatively to the two proteins by utilizing the COACH-D web-server [32].

The docking results predicted binding energy of −6.5 kcal/mol for compound **16** against IAPP. A detailed examination of the binding site allowed identifying key interacting residues, as shown in Fig. 6.

To comprehend and provide information concerning mixed-type inhibition property of compound **16** against the α-glucosidase protein, docking for the complex was also performed (Fig. 7).

In a mixed-type inhibition, the ligand binds to an allosteric protein site, which is different from the active site [39] (Fig. 7A). Indeed, the predicted binding site for compound **16** (with a binding energy value of −7.5 kcal/mol) was noted in the region different from the active site (Fig. 7B), in agreement with the kinetic binding data. Moreover, we observed a rich protein-ligand interaction network (Fig. 7C) mediated by H-bonds interactions (between hydroxyl groups of the ligand and residues Glu304, Thr307), and H-phobic interactions (Lys155, Phe157) and pi-stacking interactions (Phe157, His239) (Fig. 7D).

An important aim during early drug development is to identify promising compounds as well as to investigate their pharmacokinetics parameters [40,41]. Therefore, the presence of pan-assay interference compounds (PAINS) and the conformity to Lipinski's rule was investigated by utilizing free web tool Swiss ADME [42] (see ESI† Table S1). Furthermore, we employed a novel Brain Or IntestinaLEstimateD permeation (BOILED-Egg) method to predict simultaneously two crucial

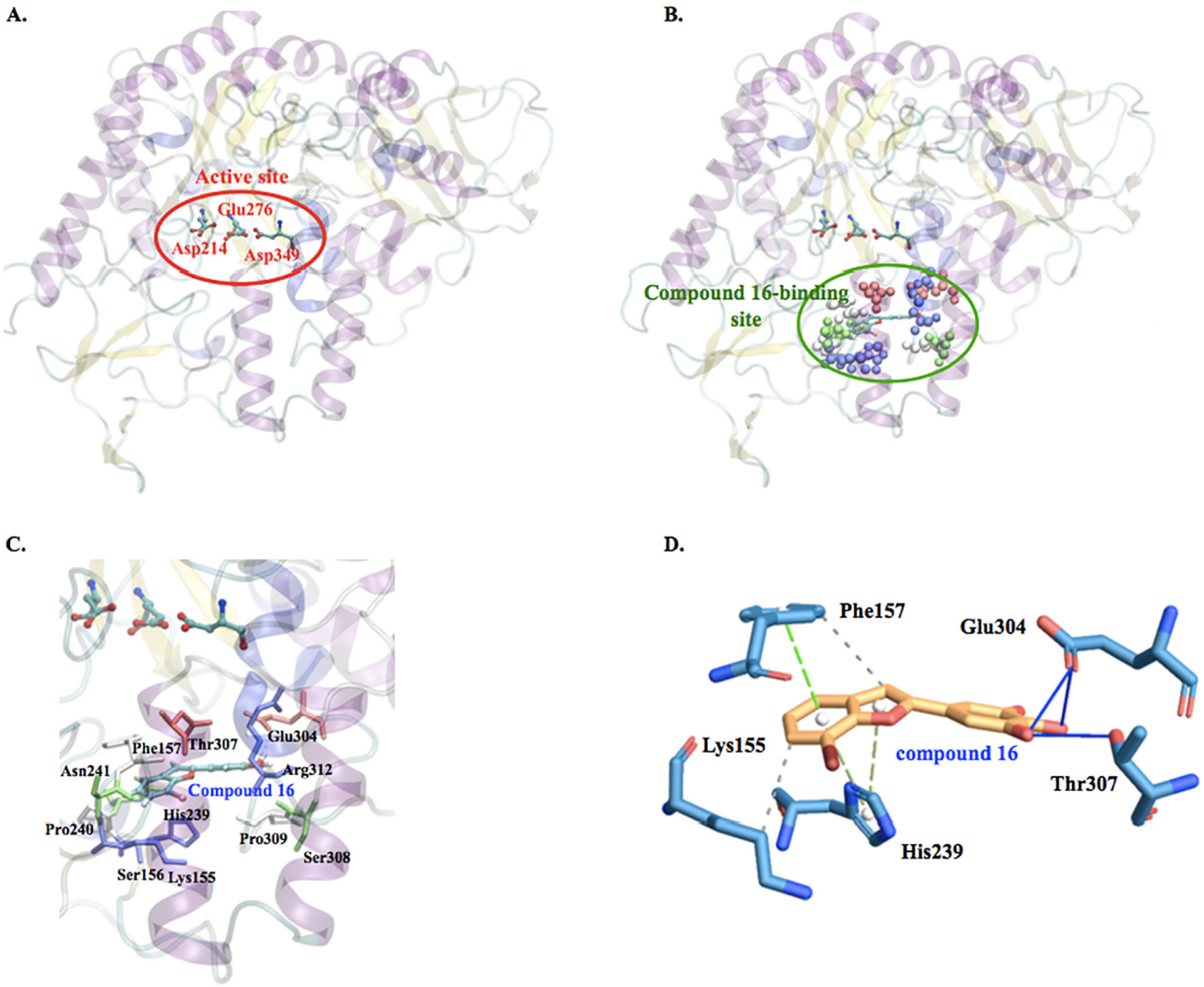

Fig. 7. Modelling α-glucosidase - compound **16** complex. A. 3D model of protein (as a cartoon), catalytic residues (as licorice), and active site highlighted in red. B. Compound **16** binding region identified from docking. C. The zoomed view of predicted ligand binding site. D. Compound **16** interactions with the protein residues mediated by H-bonds (blue), H-phobic contacts (dashed grey lines), parallel pi-stacking (green dashed line), and perpendicular pi-stacking (dark green dashed line), obtained using PLIP program [38].

pharmacokinetic parameters, namely gastrointestinal absorption (GA) and brain penetration (BA), employing two important physicochemical descriptors (lipophilicity and polarity) of compound **16** (see ESI† Fig. S3).

4. Conclusions

A series of benzofuran derivatives were efficiently synthesized, and they showed excellent inhibitory activities against α-glucosidase in comparison to the standard drug. Among these derivatives, compound **16** was the most potent one with an IC_{50} value of 0.83 ± 0.16 μM. The kinetic analysis showed that it inhibited α-glucosidase activity with a mixed-type mechanism.

The present studies provide experimental support for the action of compound **16** in preventing amyloid fibril formation. Our results highlighted a relationship between the number of hydroxyl groups and their position in the 2-phenylbenzofuran scaffold and α-glucosidase inhibitory activity.

Furthermore, docking studies revealed that the ligand-binding region is located far from the active site, thus supporting the mixed-type inhibitory characteristic of compound **16** against the α-glucosidase protein.

Overall, the findings obtained from the present study will encourage us to continue our efforts towards optimising the pharmacological profile of the 2-phenylbenzofuran derivatives. Considering that a single molecule can modulate multiple targets simultaneously is potentially a more advantageous treatment strategy than a drug cocktail for multifactorial diseases like diabetes.

CRediT authorship contribution statement

Giovanna L. Delogu: Methodology, Investigation, Writing - review & editing, Visualization **Benedetta Era**: Conceptualization, Methodology, Investigation, Writing - review & editing, Visualization **Sonia Floris**: Investigation, review & editing **Rosaria Medda**: Methodology, Review & editing **Valeria Sogos**: Methodology, Investigation **Francesca Pintus**: Methodology, Review & editing **Gianluca Gatto**: Funding acquisition, Resources **Amit Kumar**: Methodology, Investigation, Writing - review & editing, Data Curation **Gunilla Torstensdotter Westermark**: Methodology, Investigation, Funding acquisition **Antonella Fais**: Conceptualization, Methodology, Investigation, Writing - Original Draft, Visualization, Supervision.

Declaration of competing interest

The authors declare that they have no known competing financial interests or personal relationships that could have appeared to influence the work reported in this paper.

Acknowledgment

The present work was partially supported by FIR (Fondo Integrativo per la Ricerca), University of Cagliari, and by the Novo Nordisk (grant number: NNF 180c0034256) and Swedish Diabetes Foundation (grant number: DIA 2017-296) to GTW.

Appendix A. Supplementary data

Supplementary data to this article can be found online at https://doi.org/10.1016/j.ijbiomac.2020.12.117.

References

[1] H.A. Hamid, M.M. Yusoff, M. Liu, M.R. Karim, α-Glucosidase and α-amylase inhibitory constituents of Tinospora crispa: isolation and chemical profile confirmation by ultra-high performance liquid chromatography-quadrupole time-of-flight/mass spectrometry, J. Funct. Foods 16 (2015) 74–80.

[2] S. Imran, M. Taha, N.H. Ismail, S.M. Kashif, F. Rahim, W. Jamil, H. Wahab, K.M. Khan, Synthesis, in vitro and docking studies of new flavone ethers as α-glucosidase inhibitors, Chem. Biol. Drug Des. 87(3) (2016) 361–373.

[3] M. Nawaz, M. Taha, F. Qureshi, N. Ullah, M. Selvaraj, S. Shahzad, S. Chigurupati, A. Waheed, F.A. Almutairi, Structural elucidation, molecular docking, alpha-amylase and alpha-glucosidase inhibition studies of 5-amino-nicotinic acid derivatives, BMC Chem 14(1) (2020) 43.

[4] F. Rahim, M. Taha, N. Iqbal, S. Hayat, F. Qureshi, I. Uddin, K. Zaman, A. Rab, A. Wadood, N. Uddin, M. Nawaz, S.A.A. Shah, K.M. Khan, Isatin based thiosemicarbazide derivatives as potential inhibitor of α-glucosidase, synthesis and their molecular docking study, J. Mol. Struct. 1222 (2020).

[5] M. Solangi, Kanwal, K. Mohammed Khan, F. Saleem, S. Hameed, J. Iqbal, Z. Shafique, U. Qureshi, Z. Ul-Haq, M. Taha, S. Perveen, Indole acrylonitriles as potential antihyperglycemic agents: synthesis, α-glucosidase inhibitory activity and molecular docking studies, Bioorg. Med. Chem. 28(21) (2020).

[6] A.C. Maritim, R.A. Sanders, J.B. Watkins, Diabetes, oxidative stress, and antioxidants: a review, J. Biochem. Mol. Toxicol. 17 (1) (2003) 24–38.

[7] J.W.M. Höppener, F.H. Epstein, B. Ahrén, C.J.M. Lips, Islet amyloid and type 2 diabetes mellitus, New Engl. J. Med. 343(6) (2000) 411–419.

[8] J.F. Paulsson, A. Andersson, P. Westermark, G.T. Westermark, Intracellular amyloid-like deposits contain unprocessed pro-islet amyloid polypeptide (proIAPP) in beta cells of transgenic mice overexpressing the gene for human IAPP and transplanted human islets, Diabetologia 49 (6) (2006) 1237–1246.

[9] P. Westermark, C. Wernstedt, E. Wilander, K. Sletten, A novel peptide in the calcitonin gene related peptide family as an amyloid fibril protein in the endocrine pancreas, Biochem. Biophys. Res. Commun. 140 (3) (1986) 827–831.

[10] G.T. Westermark, L. Krogvold, K. Dahl-Jørgensen, J. Ludvigsson, Islet amyloid in recent-onset type 1 diabetes—the DiViD study, Ups. J. Med. Sci. 122 (3) (2017) 201–203.

[11] P. Westermark, A. Andersson, G.T. Westermark, Islet amyloid polypeptide, islet amyloid, and diabetes mellitus, Physiol. Rev. 91 (3) (2011) 795–826.

[12] L.M. Young, J.C. Saunders, R.A. Mahood, C.H. Revill, R.J. Foster, L.-H. Tu, D.P. Raleigh, S.E. Radford, A.E. Ashcroft, Screening and classifying small-molecule inhibitors of amyloid formation using ion mobility spectrometry–mass spectrometry, Nat. Chem. 7 (1) (2014) 73–81.

[13] O. Bolarinwa, C. Li, N. Khadka, Q. Li, Y. Wang, J. Pan, J. Cai, γ-AApeptides–based small molecule ligands that disaggregate human islet amyloid polypeptide, Sci. Rep. 10 (1) (2020).

[14] Y.-h. Miao, Y.-h. Hu, J. Yang, T. Liu, J. Sun, X.-j. Wang, Natural source, bioactivity and synthesis of benzofuran derivatives, RSC Adv. 9 (47) (2019) 27510–27540.

[15] M. L. Bolognesi, Polypharmacology in a single drug: multitarget drugs, Curr. Med. Chem. 20 (13) (2013) 1639–1645.

[16] M.L. Bolognesi, A. Cavalli, Multitarget drug discovery and polypharmacology, ChemMedChem 11 (12) (2016) 1190–1192.

[17] G.L. Delogu, M.J. Matos, M. Fanti, B. Era, R. Medda, E. Pieroni, A. Fais, A. Kumar, F. Pintus, 2-Phenylbenzofuran derivatives as butyrylcholinesterase inhibitors: synthesis, biological activity and molecular modeling, Bioorg. Med. Chem. Lett. 26 (9) (2016) 2308–13.

[18] A. Kumar, F. Pintus, A. Di Petrillo, R. Medda, P. Caria, M.J. Matos, D. Vina, E. Pieroni, F. Delogu, B. Era, G.L. Delogu, A. Fais, Novel 2-pheynlbenzofuran derivatives as selective butyrylcholinesterase inhibitors for Alzheimer's disease, Sci. Rep. 8(1) (2018) 4424.

[19] A. Fais, A. Kumar, R. Medda, F. Pintus, F. Delogu, M.J. Matos, B. Era, G.L. Delogu, Synthesis, molecular docking and cholinesterase inhibitory activity of hydroxylated 2-phenylbenzofuran derivatives, Bioorg. Chem. 84 (2019) 302–308.

[20] J.-F. Hsieh, W.-J. Lin, K.-F. Huang, J.-H. Liao, M.-J. Don, C.-C. Shen, Y.-J. Shiao, W.-T. Li, Antioxidant activity and inhibition of α-glucosidase by hydroxyl-functionalized 2-arylbenzo[b]furans, Eur. J. Med. Chem. 93 (2015) 443–451.

[21] I. Ali, R. Rafique, K.M. Khan, S. Chigurupati, X. Ji, A. Wadood, A.U. Rehman, U. Salar, M.S. Iqbal, M. Taha, S. Perveen, B. Ali, Potent alpha-amylase inhibitors and radical (DPPH and ABTS) scavengers based on benzofuran-2-yl(phenyl)methanone derivatives: syntheses, in vitro, kinetics, and in silico studies, Bioorg. Chem. 104 (2020), 104238, .

[22] J. Madhusudhanan, G. Suresh, V. Devanathan, Neurodegeneration in type 2 diabetes: Alzheimer's as a case study, Brain and Behavior 10 (5) (2020).

[23] A. Fais, B. Era, A. Di Petrillo, S. Floris, D. Piano, P. Montoro, C.I.G. Tuberoso, R. Medda, F. Pintus, Selected enzyme inhibitory effects of Euphorbia characias extracts, Biomed. Res. Int. 2018 (2018) 1–9.

[24] R.P.R. Nanga, J.R. Brender, S. Vivekanandan, A. Ramamoorthy, Structure and membrane orientation of IAPP in its natively amidated form at physiological pH in a membrane environment, Biochim. Biophys. Acta Biomembr. 1808 (10) (2011) 2337–2342.

[25] A. Waterhouse, M. Bertoni, S. Bienert, G. Studer, G. Tauriello, R. Gumienny, F.T. Heer, T.A P. de Beer, C. Rempfer, L. Bordoli, R. Lepore, T. Schwede, SWISS-MODEL: homology modelling of protein structures and complexes, Nucleic Acids Res.. 46(W1) (2018) W296-W303.

[26] K. Yamamoto, H. Miyake, M. Kusunoki, S. Osaki, Crystal structures of isomaltase from Saccharomyces cerevisiae and in complex with its competitive inhibitor maltose, FEBS J. 277 (20) (2010) 4205–4214.

[27] T. Luthra, V. Banothu, U. Adepally, K. Kumar, S. M, S. Chakrabarti, S.R. Maddi, S. Sen, Discovery of novel pyrido-pyrrolidine hybrid compounds as alpha-glucosidase inhibitors and alternative agent for control of type 1 diabetes, Eur. J. Med. Chem. 188 (2020).

[28] P. Benkert, M. Biasini, T. Schwede, Toward the estimation of the absolute quality of individual protein structure models, Bioinformatics 27 (3) (2011) 343–350.

[29] N.M. O'Boyle, M. Banck, C.A. James, C. Morley, T. Vandermeersch, G.R. Hutchison, Open babel: an open chemical toolbox, Journal of Cheminformatics 3 (1) (2011).
[30] A. Kumar, R. Baccoli, A. Fais, A. Cincotti, L. Pilia, G. Gatto, Substitution effects on the optoelectronic properties of Coumarin derivatives, Appl. Sci. 10(1) (2020).
[31] A. Di Petrillo, C. Santos-Buelga, B. Era, A.M. Gonzalez-Paramas, C.I.G. Tuberoso, R. Medda, F. Pintus, A. Fais, Sardinian honeys as sources of xanthine oxidase and tyrosinase inhibitors, Food Sci. Biotechnol. 27 (1) (2018) 139–146.
[32] Q. Wu, Z. Peng, Y. Zhang, J. Yang, COACH-D: improved protein-ligand binding sites prediction with refined ligand-binding poses through molecular docking, Nucleic Acids Res. 46 (W1) (2018) W438–W442.
[33] A. Hercouet, M. Le Corre, Une nouvelle voie d'accès aux benzofurannes, Tetrahedron Lett. 20 (23) (1979) 2145–2148.
[34] M. Begala, P. Caboni, M.J. Matos, G.L. Delogu, Unexpected one-step synthesis of 3-benzoyl-2-phenylbenzofurans under Wittig conditions, Tetrahedron Lett. 59 (18) (2018) 1711–1714.
[35] M. Begala, M. Mancinelli, G.L. Delogu, Unexpected migration of a benzoyl group in the intramolecular Wittig reaction of o-acyloxybenzylidenephosphoranes with benzoyl chlorides: one-pot synthesis of isomeric 3-benzoyl-2-phenylbenzofurans, Tetrahedron Lett. 61 (12) (2020).
[36] P. Attri, K.Y. Baik, P. Venkatesu, I.T. Kim, E.H. Choi, Influence of hydroxyl group position and temperature on thermophysical properties of tetraalkylammonium hydroxide ionic liquids with alcohols, PLoS One 9 (1) (2014).
[37] R.A. Laskowski, M.B. Swindells, LigPlot+: multiple ligand–protein interaction diagrams for drug discovery, J. Chem. Inf. Model. 51 (10) (2011) 2778–2786.
[38] S. Salentin, S. Schreiber, V.J. Haupt, M.F. Adasme, M. Schroeder, PLIP: fully automated protein–ligand interaction profiler, Nucleic Acids Res. 43 (W1) (2015) W443–W447.
[39] S. Floris, A. Fais, A. Rosa, A. Piras, H. Marzouki, R. Medda, A.M. González-Paramás, A. Kumar, C. Santos-Buelga, B. Era, Phytochemical composition and the cholinesterase and xanthine oxidase inhibitory properties of seed extracts from the Washingtonia filifera palm fruit, RSC Adv. 9 (37) (2019) 21278–21287.
[40] U. Ammarah, A. Kumar, R. Pal, N.C. Bal, G. Misra, Identification of new inhibitors against human Great wall kinase using in silico approaches, Sci. Rep. 8 (1) (2018), 4894, .
[41] B. Era, G.L. Delogu, F. Pintus, A. Fais, G. Gatto, E. Uriarte, F. Borges, A. Kumar, M.J. Matos, Looking for new xanthine oxidase inhibitors: 3-Phenylcoumarins versus 2-phenylbenzofurans, Int. J. Biol. Macromol. 162 (2020) 774–780.
[42] A. Daina, O. Michielin, V. Zoete, SwissADME: a free web tool to evaluate pharmacokinetics, drug-likeness and medicinal chemistry friendliness of small molecules, Sci. Rep. 7 (1) (2017).